SPECIAL PROJECT PROGRESS REPORT

All the following mandatory information needs to be provided. The length should *reflect the complexity and duration* of the project.

Reporting year

2020

Project Title:

Deep Vertical Propagation of Internal Gravity Waves

Computer Project Account:

SPDESCAN

Principal Investigator(s):

Dr. Andreas Dörnbrack
Dr. Sonja Gisinger
Dr. Andreas Schäfler
Dr. Klaus-Peter Hoinka

Affiliation:

DLR Oberpfaffenhofen
Institut für Physik der Atmosphäre
Münchener Str. 20

D – 82230 WESSLING

Germany

Name of ECMWF scientist(s) collaborating to the project
(if applicable)

Dr. Nils Wedi
Dr. Inna Polichtchouk
Dr. Christian Kühnlein
Dr. Peter Bechthold
Dr. Piotr K Smolarkiewicz

Start date of the project:

1 January 2018

Expected end date:

2020

Computer resources allocated/used for the current year and the previous one

(if applicable)
Please answer for all project resources

		Previous year		Current year	
		Allocated	Used	Allocated	Used
High Performance Computing Facility	(units)	500000	500000	500000	200000
Data storage capacity	(Gbytes)	80	80	80	80

Summary of project objectives (10 lines max)

During the recent years, ground-based and airborne Rayleigh lidar measurements of temperature perturbations in the middle atmosphere show gravity wave activity covering a large spectrum of frequencies and vertical and horizontal wavelengths. An understanding of the different wave modes in the middle atmosphere is still lacking. Especially, the link of the observed gravity wave activity to possible sources in the troposphere as well as in the stratosphere is difficult to establish as 3D data of wind and temperature in high spatial and temporal resolution are missing. Therefore, the integrated forecast system (IFS) of the ECMWF will serve to fill this gap by providing these data globally. Idealized numerical simulations will complement the combined analysis of data and IFS output.

Summary of problems encountered (10 lines max)

No problems encountered.

Summary of plans for the continuation of the project (10 lines max)

As this project will be terminated, a new one will be proposed in a similar spirit.

List of publications from the project with complete references

1. **Bramberger, M**., **A. Dörnbrack**, H. Wilms, F. Ewald, and R. Sharman, 2020: Mountain-Wave Turbulence Encounter of the Research Aircraft HALO above Iceland. *J. Appl. Meteor. Climatol.*, **59**, 567–588, https://doi.org/10.1175/JAMC-D-19-0079.1

2. Eckermann, S.D., J.D. Doyle, P.A. Reinecke, C.A. Reynolds, R.B. Smith, D.C. Fritts, and **A. Dörnbrack**, 2019: Stratospheric Gravity Wave Products from Satellite Infrared Nadir Radiances in the Planning, Execution, and Validation of Aircraft Measurements during DEEPWAVE. *J. Appl. Meteor. Climatol.*, **58**, 2049–2075, https://doi.org/10.1175/JAMC-D-19-0015.1

3. Egger, J. and **K.-P. Hoinka**, 2020: Piecewise potential vorticity inversion without far-field response? *J. Atmos. Sci.*, submitted.

4. Fritts, D. C., Miller, A. D., Kjellstrand, C. B., Geach, C., Williams, B. P., Kaifler, B., Kaifler, N, Jones, G., Rapp, M., Limon, M., Reimuller, J., Wang, L., Hanany, S., **Gisinger, S**., Zhao, Y., Stober, G., and C. E. Randall, 2019: PMC Turbo: Studying gravity wave and instability dynamics in the summer mesosphere using polar mesospheric cloud imaging and profiling from a stratospheric balloon. *Journal of Geophysical Research: Atmospheres*, **124,** 6423– 6443. https://doi.org/10.1029/2019JD030298

5. Heale, C. J., Bossert, K., Vadas, S. L., Hoffmann, L., **Dörnbrack, A**., Stober, G., and J. B. Snively , and C. Jacobi, 2020: Secondary gravity waves generated by breaking mountain waves over Europe. *Journal of Geophysical Research: Atmospheres*, 125, e2019JD031662. https://doi.org/10.1029/2019JD031662

6. **Schäfler, A**., B. Harvey, J. Methven, J. D. Doyle, S. Rahm, O. Reitebuch, F. Weiler, and B. Witschas, 2020: Observation of Jet Stream Winds during NAWDEX and Characterization of Systematic Meteorological Analysis Errors. *Mon. Wea. Rev.*, **148**, 2889–2907, https://doi.org/10.1175/MWR-D-19-0229.1.

7. **Schäfler, A.,** G. Craig, H. Wernli, P. Arbogast, J.D. Doyle, R. McTaggart-Cowan, J. Methven, G. Rivière, F. Ament, M. Boettcher, **M. Bramberger**, Q. Cazenave, R. Cotton, S. Crewell, J. Delanoë, **A. Dörnbrack**, A. Ehrlich, F. Ewald, A. Fix, C.M. Grams, S.L. Gray, H. Grob, S. Groß, M. Hagen, B. Harvey, L. Hirsch, M. Jacob, T. Kölling, H. Konow, C. Lemmerz, O. Lux, L. Magnusson, B. Mayer, M. Mech, R. Moore, J. Pelon, J. Quinting, S. Rahm, M. Rapp, M. Rautenhaus, O. Reitebuch, C.A. Reynolds, H. Sodemann, T. Spengler, G. Vaughan, M. Wendisch, M. Wirth, B. Witschas, K. Wolf, and T. Zinner, 2018: The North Atlantic Waveguide and Downstream Impact Experiment. *Bull. Amer. Meteor. Soc.*, **99**, 1607–1637, https://doi.org/10.1175/BAMS-D-17-0003.1.

8. Wilms, H., **Bramberger, M**., and **A. Dörnbrack**, 2020: Observation and Simulation of Mountain Wave Turbulence above Iceland: Turbulence Intensification due to Wave Interference. *Q. J. R. Met. Soc.*, accepted 8 June 2020; doi:10.1002/qj.3848

9. Woiwode, W., **Dörnbrack, A**., Polichtchouk, I., Johansson, S., Harvey, B., Höpfner, M., Ungermann, J., and Friedl-Vallon, F.: Technical note: Lowermost-stratospheric moist bias in ECMWF IFS model diagnosed from airborne GLORIA observations during winter/spring 2016, Atmos. Chem. Phys. Discuss., https://doi.org/10.5194/acp-2020-367, in review, 2020.

Summary of results

(1) Usage of IFS data for airborne field campaigns

The ECMWF operational forecast data from the Integrated Forecasting System (IFS) have been used extensively for mission and flight planning during field campaigns, especially, for airborne platforms conducted with the German research aircraft HALO and DLR Falcon around the globe. The focus of the different missions covered a broad spectrum of different topics such as trace gas emissions and pollution of mega cities in Europe and East-Asia (EMeRGe[1], COMET[2]) as well as atmospheric dynamics and transport in the North Atlantic region (NAWDWEX[3]) and the Southern Hemisphere high latitudes (SouthTRAC[4]).

The different mission topics, used instruments, and the specific conditions in the area of operations (e.g., local weather, instructions by local authorities for handling flight plans,…) define the requirements of the forecasts. For example, forecasting the transport of trace gases by tropospheric winds and finding an area with mostly cloud-free conditions, where they can be measured by the instruments onboard, was the most important aspect during the EMeRGe campaign. During the SouthTRAC campaign, the focus was on forecasting of the occurrence of internal gravity waves in the stratosphere and mesosphere in the region of the Southern Andes, the Drake Passage, and the Antarctic Peninsula and on forecasting the polar vortex position.

[1] Effect of Megacities on the Transport and Transformation of Pollutants on the Regional to Global Scales, see https://www.halo.dlr.de/science/missions/emerge/emerge.html
[2] Carbon Dioxide and Methane Mission, https://www.halo.dlr.de/science/missions/comet/comet.html
[3] North Atlantic Waveguide and Downstream impact Experiment, Schäfler et al. (2018)
[4] https://www.pa.op.dlr.de/southtrac/science/introduction/

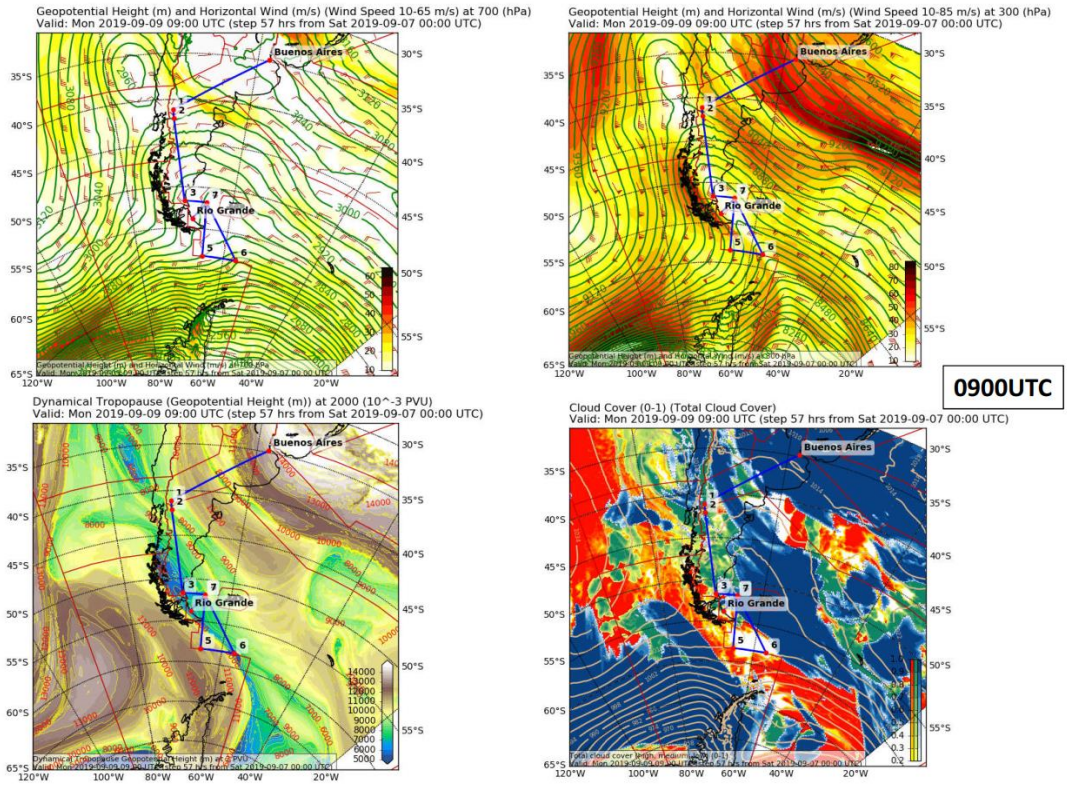

Figure 1: Horizontal maps of horizontal wind at 700 and 300 hPa, height of the dynamical tropopause, and cloud cover created with the mission support system during the SouthTRAC campaign. Flight tracks and waypoints are also shown in these maps.

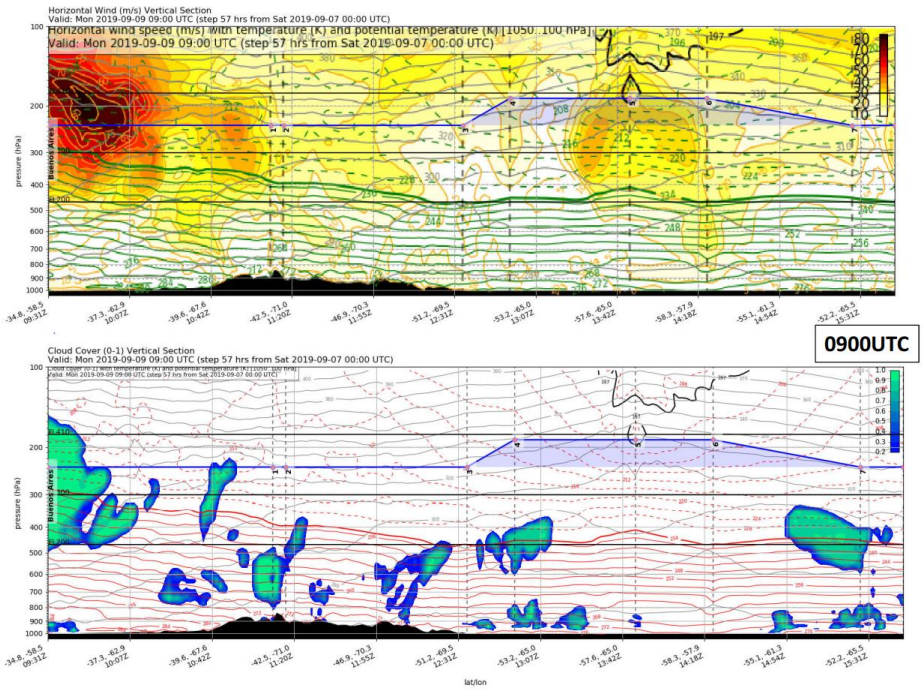

Figure 2: Vertical cross section of horizontal wind and cloud cover created with the mission support system along the flight track shown in Fig.1.

For these different purposes, ECMWF operational forecasts were visualized on a website showing the required forecast parameters. Moreover, the forecast data were integrated and visualized with the Mission Support System[5] which allows for creating horizontal maps of different parameters (Fig. 1) and vertical cross sections along flight tracks (Fig. 2). The common visualization of different forecast products by this tool is essential for the effective flight planning during aircraft field campaigns. Moreover, the most recent available forecasts along the final flight path provide guidance for the scientists on board for inflight decisions (e.g., change of altitude,…).

(2) Observation of jet stream winds during NAWDEX and characterization of systematic meteorological analysis errors (Schäfler et al., 2020)

Operational analysis and forecast data from the ECMWF's IFS and UK MetOffice Unified Model were applied in combination with high vertical resolution wind observations to explore the structure of the North Atlantic jet stream, including the sharpness of vertical wind shear changes across the tropopause and the wind speed (Schäfler et al., 2020). This study was conducted in the context of the North Atlantic Waveguide and Downstream impact EXperiment (NAWDEX). Airborne Doppler wind lidar, dropsonde and a ground-based stratosphere-troposphere radar data revealed small wind speed biases throughout the troposphere and lower stratosphere. However, this study finds large and spatially coherent wind errors up to ±10 m s^{-1} for individual cases, with the strongest errors occurring above the tropopause in upper-level ridges.

Figure 3 shows an example of observed wind speeds and respective differences across a jet stream that was observed between Iceland and the UK on 23 November 2016.

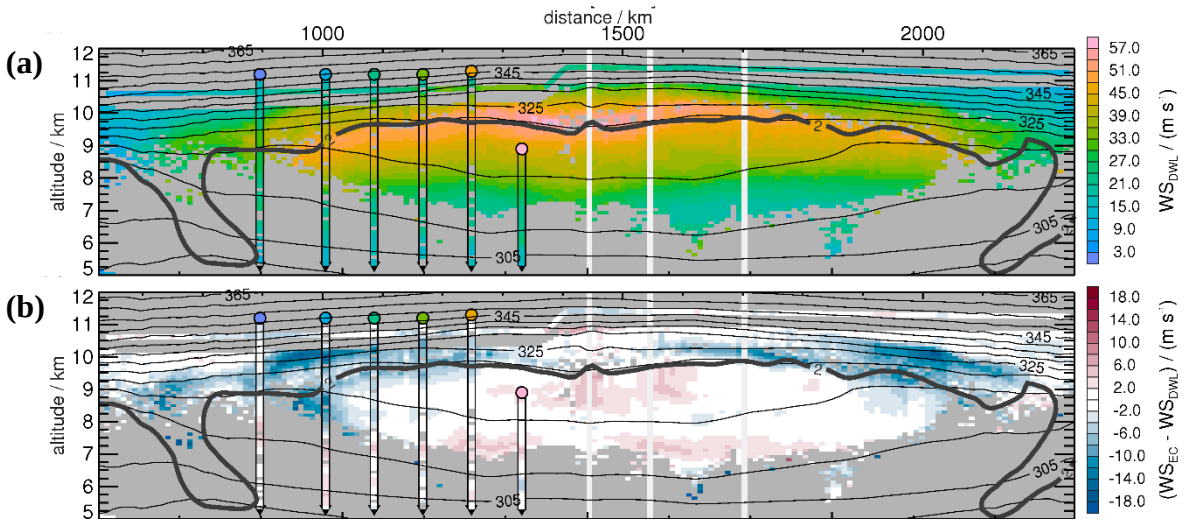

Figure 3: (a) Doppler wind lidar (colored areas), dropsonde (colored observations along arrows) and in situ (colored line contour on top of wind lidar observations) wind observations and (b) the respective differences to short-range forecast fields of the ECMWF IFS on 23 Oct 2016. (a, b) are superimposed by potential temperature (black contours) and dynamical tropopause (2 PVU, thick black contour) from. Figure taken from Schäfler et al. (2020).

[5] https://mss.readthedocs.io/en/stable/installation.html

ECMWF and Met Office analyses indicate similar spatial structures in wind errors, even though their forecast models and data assimilation schemes differ greatly. The assimilation of operational observational data brings the analyses closer to the independent verifying observations but it cannot fully compensate the forecast error. Models tend to underestimate the peak jet stream wind, the vertical wind shear (by a factor of 2…5), and the abruptness of the change in wind shear across the tropopause, which is a major contribution to the meridional potential vorticity gradient. The differences are large enough to influence forecasts of Rossby wave disturbances to the jet stream with an anticipated effect on weather forecast skill even on large scales.

(3) Observation and Simulation of Mountain Wave Turbulence above Iceland: Turbulence Intensification due to Wave Interference (Wilms et al., 2020)

The High Altitude LOng Range research aircraft (HALO) encountered strong turbulence above Iceland at 13.8 km altitude on October 13, 2016. The generation of turbulence along the flight path is studied through numerical simulations in combination with the aircraft in situ observations. From the in situ observations, maximum EDR values (cubic root of the energy dissipation rate) of 0.39 $m^{2/3}$ s^{-1} are obtained, which correspond to moderate to severe turbulence for a medium-weight aircraft such as HALO. The turbulent region is characterized by observed large amplitude vertical wind fluctuations which coincide locally with a stagnation of the horizontal flow.

The strong turbulence occurred downstream and in between the two Icelandic mountains Hofsjökull and Langjökull. High-resolution numerical simulations, with realistic and idealized topography, show that the flow above these two nearby mountains is responsible for the observed turbulence.

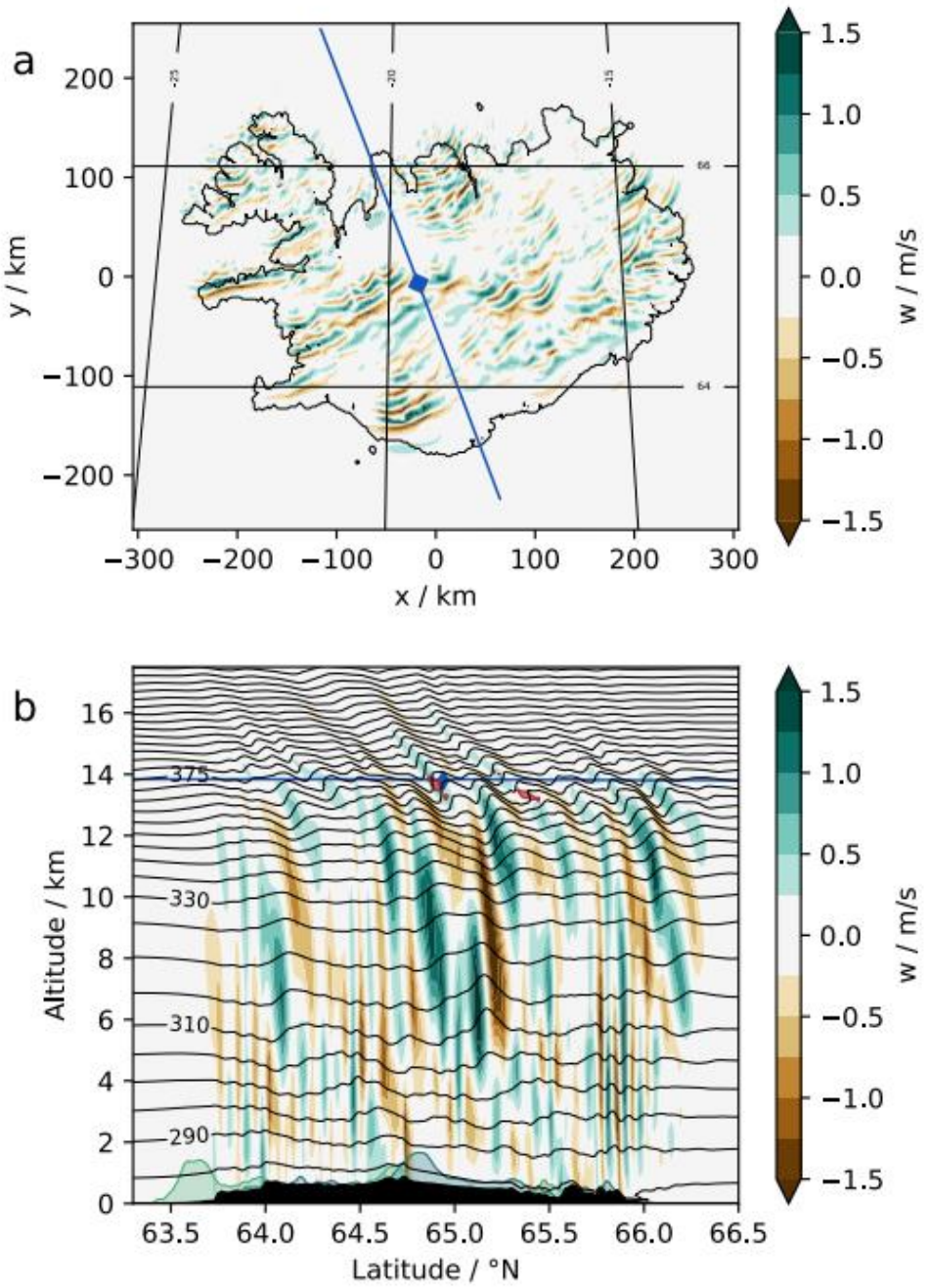

Figure 4: (a) Horizontal cross section of *w* from Iceland 3D simulation at 13 km altitude at *t* = 0:75 h. (b) Cross section along HALO flight track of *w* (color) and isentropes (black contours, in K) at *t* = 1:75 h. The blue line indicates the flight track with the turbulence encounter at the position of the filled blue diamond. The thin black lines in (a) denote longitude and latitude. In (b) red shaded regions indicate where $N^2 < 0$. The black filled area is the topography along the flight track, the blue and green filled areas are the topography along cross sections parallel to the flight track cutting through the peak of Hofsjökull and Langjökull.

Vertically propagating hydrostatic mountain waves disperse horizontally in the region downstream and in between Hofsjökull and Langjökull. There, both waves interfere and their superposition leads to enhanced amplitudes and, eventually, to convective instabilities. By comparing simulations with only one of the mountains to the simulation with both mountains, we infer that the wave

interference can locally amplify the turbulence intensity by a factor of five and double the vertical extent of the turbulent region.

(4) Lidar observations of large-amplitude mountain waves in the stratosphere above Tierra del Fuego, Argentina (Kaifler et al., 2020)

Large-amplitude internal gravity waves were observed using Rayleigh lidar temperature soundings above Rio Grande, Argentina (54°S, 68°W), in the period 16…23 June 2018. Temperature perturbations in the upper stratosphere amounted to 80 K peak-to-peak and potential energy densities exceeded 400 J/kg. The measured amplitudes and phase alignments agree well with operational analyses and short-term forecasts of the IFS implying that these quasi-steady gravity waves resulted from the airflow across the Andes. We estimate gravity wave momentum fluxes larger than 100 mPa applying independent methods to both lidar data and IFS model data. These mountain waves deposited momentum at the inner edge of the polar night jet and led to a long-lasting deceleration of the stratospheric flow. The accumulated mountain wave drag affected the stratospheric circulation several thousand kilometers downstream. In the 2018 austral winter, mountain wave events of this magnitude contributed more than 30 % of the total potential energy density, signifying their importance by perturbing the stratospheric polar vortex.

(6) Far-ranging impact of mountain waves excited over Greenland on stratospheric dehydration and rehydration (Kivi et al., 2020)

In situ observations of reduced stratospheric water vapor combined with those of ice particle formation are rarely conducted. On the one hand, they are essential to broaden our knowledge about the formation of polar stratospheric clouds (PSCs). On the other hand, the observed profiles allow the comparison with global circulation models. Here, we report about a balloon-borne observation above Sodankylä, Finland on 26 January 2005. The frostpoint hygrometer detected layers of reduced water vapor by up to 2 ppmv from 18.5 to 23 km. Beneath, a 1 km deep layer of increased water vapor was identified. An aerosol backscatter sonde measured the presence of stratospheric ice clouds.

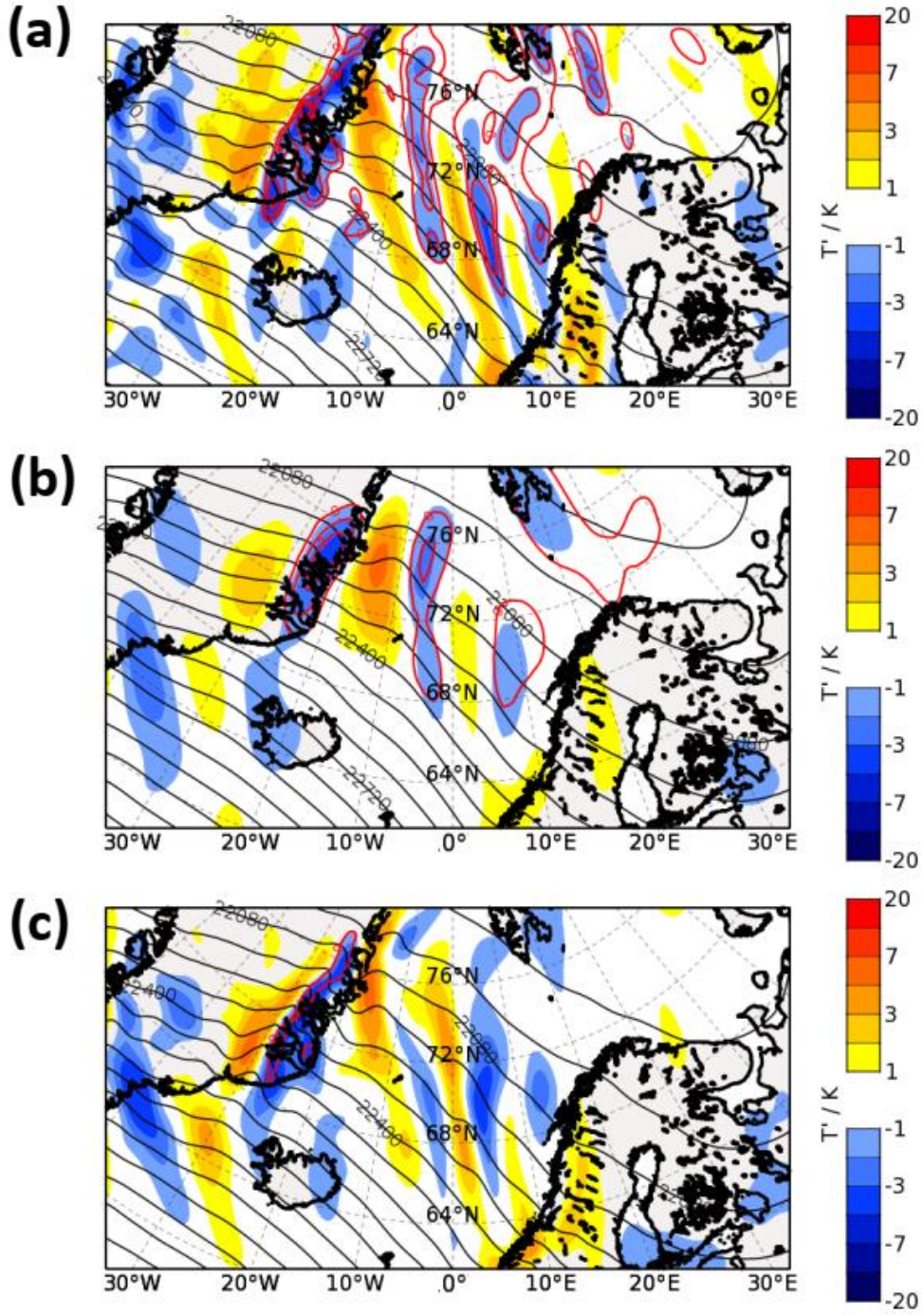

Figure 5. Temperature perturbations T' (K, color shaded) at 30 hPa on 26 January 2005 06 UTC from ERA5 (a), ERA Interim (b), and the operational ECMWF T511/L60 analyses (c). The red encircled areas are regions where ice clouds are likely to exist. In all panels: geopotential height (m, increment 80 m, black solid lines) and $T\text{-}T_{ICE} \leq 0$ (red solid lines, interval 1 K).

According to meteorological analysis the PSCs were formed upstream above the east coast of Greenland due to mountain wave-induced cooling. The mountain wave-induced temperature perturbations spread over the whole Atlantic Ocean and lead to the observed dehydration. Comparing the most recent ERA5 data with operational analyses from 2005, we find an improved representation of mesoscale internal gravity waves, of dehydration, and of PSC formation for this particular event.